JAEHR
Journal of Advances in Environmental Health Research
J Adv Environ Health Res, 2023; 11(2): 94-105. doi: 10.34172/jaehr.2023.12
http://jaehr.muk.ac.ir

Original Article

Photocatalytic Degradation of Cefixime Antibiotic by Polyaniline/SnO_2 Nanocomposite and Optimization of the Process Using Response Surface Methodology

Parishan Salih Mohammed, Kambiz Seyyedi*

Department of Chemistry, Tabriz branch, Islamic Azad University, Tabriz 5157944533, Iran

Article history:
Received: May 28, 2022
Accepted: September 24, 2022
ePublished: July 16, 2023

***Corresponding author:**
Kambiz Seyyedi,
Email: k.seyyedi@iaut.ac.ir

Abstract

Background: Aniline-based organic nanocomposites have a significant performance as photocatalysts in the advanced oxidation process (AOP).

Methods: In this study, polyaniline-tin dioxide (PA/SnO_2) nanocomposite was prepared using an ultrasonic process. Next, its efficiency as a photocatalyst in the removal of Cefixime antibiotic pollutant from contaminated waters in a tubular photo reactor was investigated. The experiments were designed by the response surface methodology (RSM) via Minitab software, in such a way that the effects of various parameters on the process are investigated. The effect of different parameters such as reaction time, solution pH, flow rate, antibiotic concentration and hydrogen peroxide concentration on the removal efficiency was investigated.

Results: According to the results, the following optimal conditions were obtained: time of 120 min, pH of 8.69, hydrogen peroxide concentration of 4.22 mM, flow rate of 1.25 L/min and initial antibiotic concentration of 22.92 mg/L. Under the above-mentioned optimal conditions, the efficiency of Cefixime removal was more than 72.24%.

Conclusion: The present study confirms the usability of the PA/SnO_2 nanocomposite as a novel and effective photocatalyst for photocatalytic degradation of Cefixime antibiotic in contaminated water under UV light.

Keywords: Degradation, Cefixime antibiotic, Photocatalytic process, Polyaniline PA/SnO_2 nanocomposite, Tubular photo reactor, Optimization, RSM

Please cite this article as follows: Salih Mohammed P, Seyyedi K. Photocatalytic degradation of Cefixime antibiotic by polyaniline/SnO_2 nanocomposite and optimization of the process using response surface methodology. J Adv Environ Health Res. 2023; 11(2):94-105. doi:10.34172/jaehr.2023.12

Introduction

In recent years, the use of antibiotics in animal and human medicine has become widespread, thus increasing the possibility of water contamination with such compounds. Among all the medicinal compounds that cause environmental pollution, antibiotics play an important role in causing pollution due to their high use in medicine and veterinary science. The problem caused by the presence of antibiotics in the environment is the development of bacterial resistance to antibiotics. In recent years, there has been a significant increase in the prevalence of bacterial resistance to antibiotics, which many researchers attribute to the overuse of antibiotics.[1,2] Many wastewater treatment plants are not designed to treat wastewater containing pharmaceutical contaminants. Therefore, practical and cost-effective methods should be considered for the treatment of effluents containing antibiotics discharged into the environment, such as chemical oxidation, biodegradation, and adsorption.[3,4] The persistent nature of antibiotic-containing effluents against biodegradation has made it challenging to remove these compounds by conventional treatment methods. In these cases, the use of advanced oxidation processes (AOPs) is an important option. AOPs are oxidation methods that rely on the formation of hydroxyl intermediate radicals. These radicals are highly reactive and less selective than other oxidants. As a result, AOPs are capable of mineralizing various types of pollutants.[5,6] The photocatalytic removal of antibiotics has been investigated by using a variety of catalysts such as ZnO, TiO_2, and Fe.[7,8]

Among various AOPs, a photocatalyst using a commercial SnO_2 catalyst is widely used due to its high efficiency, chemical and physical stability, non-toxicity, and relatively inexpensive biocompatibility for water treatment. Tin oxide (SnO_2) is a very important n-type semiconductor with a relatively wide energy

gap (Eg = 3.6 eV) at room temperature, which is used in the manufacture of gas sensors, color-based solar cells, optoelectronic devices, electrode materials and photocatalyst is used.[9,10] When SnO_2 particles are exposed to radiation of photons with energy levels higher than the band gap (about 3.6 eV), electron-hole pairs (e^-/h^+) can be generated. the subsequent reaction of h + with H_2O or OH^- causes the formation of reactive radicals that act as strong oxidizing agents for the adsorbed contaminants. UV radiation (λ < 387) is required as a light source due to the higher energy gap of SnO_2.[11,12] The related equations are as follows:

$$SnO_2 + h\vartheta \rightarrow SnO_2\left(e_{CB}^- + h_{VB}^+\right)$$

$$SnO_2\left(h_{VB}^+\right) + H_2O \rightarrow SnO_2 + H^+ + OH$$

$$SnO_2\left(h_{VB}^+\right) + OH^- \rightarrow SnO_2 + OH$$

$$SnO_2\left(e_{CB}^-\right) + H_2O_2 \rightarrow OH^- + OH + SnO_2$$

$$Organic\ compound + OH \rightarrow Degradation\ products$$

$$Organic\ compound + SnO_2\left(h_{VB}^+\right) \rightarrow Oxidation\ products$$

$$Organic\ compound + SnO_2\left(e_{CB}^-\right) \rightarrow Reduction\ products$$

Despite several studies on SnO_2 photocatalysts for the optical decomposition of organic contaminants, some limitations such as separation of semiconductor powder from discontinuous slurry photoreactors and high recombination tendency of optically generated e-/h + still remain. In addition, the UV spectrum present in sunlight is very low (< 5%), which limits the use of UV and visible photocatalysts for SnO_2.[13,14]

Given the limitations and harmful effects of ultraviolet light on human life, changing the active region of ZnO, SnO_2 or TiO_2 into the visible spectrum poses a major challenge. However, this can be accomplished by modifying nanoparticles and modifying the surface by metal ion doping, non-metal doping and noble metal deposition, bonding to narrowband semiconductors, color sensitization and several other sensitizers.[2,15] Recently, the use of nanocomposites based on conductive polymers and semiconductor metal oxides has been widely considered and is an interesting research area because it has both organic and mineral properties. Conductive polymers have been reported to act as sensitizers to increase the spectral response to visible light emission of ZnO, SnO_2 and TiO_2. In this regard, sensitizers can enhance the transport of optically generated electrons.[16,17]

Conductive polymers (e.g. polyaniline, polypyrrole, and polythiophene) have been extensively studied due to their unique electrical and optical properties, including high absorption coefficient, good electron transport, high electron mobility, and excellent stability. As a commonly used polymer, polyaniline has many advantages such as low cost, high polymerization efficiency, easy synthesis, environmental resistance, and chemical resistance.[18-20]

The use of polyaniline to improve the photocatalytic activity of SnO_2 nanoparticles has been extensively studied. In the extended π-bonding system, Polyaniline enhances the optically generated charge and prevents e^-/h^+ recombination. Subsequently, the electrons can migrate to the surface of the nanocomposite and react with water and oxygen to generate hydroxyl and superoxide radicals. These radicals act as strong oxidizing agents and can effectively decompose or oxidize organic molecules.[21,22] Polyaniline, despite having unique properties such as electrical and electrochemical properties, has limitations in terms of mechanical properties and thermal stability. However, recently, organic-inorganic hybrid compounds (nanocomposites) have been highly regarded by researchers due to their properties of organic compounds and properties of minerals together and are an interesting field of research. Therefore, another solution to overcome the disadvantages of polyaniline is to prepare polyaniline nanocomposites with nanostructures, including metal oxide nanoparticles.[23]

The objective of this work was to evaluate the applicability of polyaniline-tin dioxide (PA/SnO_2) nanocomposites for the treatment of wastewater containing Cefixime antibiotic by the photocatalytic method in a recirculating tubular reactor. The effects of various parameters such as pH, concentration of antibiotic, flow rate, concentration of oxidizing reagent and process time were investigated and optimized by response surface methodology (RSM).

Materials and Methods

Materials and Photocatalytic Reactor

Hydrogen peroxide solution (30% w/w), NaOH and H_2SO_4 (to adjust the pH), HCl, aniline, ammonia, ammonium persulfate (APS), $SnCl_4$. $5H_2O$ and ethanol were provided by Merck Company. All chemicals, used for the experiments, were of analytical grade and used without further purification. The Cefixime antibiotic (85% purity) was obtained from Zahravi Pharma Co. (Iran). Distilled water was used in all steps of this work. The reactor used in this study was a recirculating tubular reactor with a diameter of 5 cm and a length of 30 cm. According to Figure 1, the system consisted of two parts: a wooden chamber in which the UV lamp (15 W, Philips) was installed and a tubular reactor made of quartz, which PA/SnO_2 nanocomposite fixed on glass (2 cm × 1 cm) was installed inside it as a photocatalyst. The solution containing cefixime antibiotic contaminant was pumped back through the reactor to remove the contaminant by the photocatalytic method. In this system, 2.5 L of cefixime antibiotic containing the necessary amount of H_2O_2 and with a specified pH was passed through the reactor. The stabilized PA/SnO_2 nanocomposite was located on the glass by a thermal stabilization method. The physicochemical properties of the antibiotic have been given in Table 1.

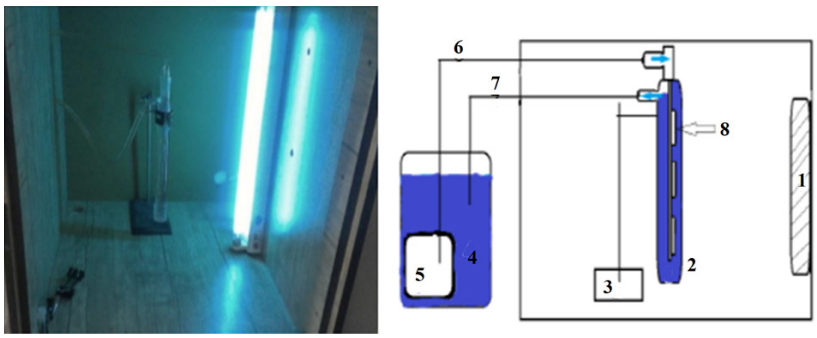

Figure 1. Schematic Image of the Setup: (1) UV Lamp, (2) Reactor, (3) Stabilizing Clip, (4) Antibiotic Solution Container, (5) Pump, (6) Interface Hose, (7) Interface Hose, (8) Photocatalyst

Table 1. Chemical structure and characteristics of Cefixime antibiotic[24]

Chemical structure	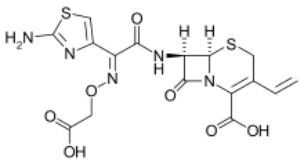
Chemical formula	$C_{16}H_{15}N_5O_7S_2$
IUPAC name	(6R,7R)-7-{[2-(2-Amino-1,3-thiazol-4-yl)-2-(carboxymethoxyimino)acetyl]amino}-3-ethenyl-8-oxo-5-thia-1-azabicyclo[4.2.0] oct-2-ene-2-carboxylic acid
Commercial name	SUPRAX, ROXIM
Molecular weight	453.44 g/mol
Drug bank	DB00671
CAS number	79350-37-1
Solubility in water (mg/L)	104

Characterization of the Equipment

UV–Vis absorption spectra were obtained by a Shimadzu 1700 Model UV–Vis spectrophotometer. The scanning electron microscopy (SEM) images of the samples were achieved using a TESCANMIRA3 model of scanning electron microscope. The following devices were used to analyze and characterization of the PA/SnO_2 nanocomposite: TEM (FEI, Tecnai F-30, USA), FTIR (Bruker Tensor 27, Germany), thermo gravimetric analysis (TGA) Mettler Toledo, Switzerland). The pH values were measured by a pH meter (Philips PW 9422). The radiation source was a low pressure mercury UV lamp (15W, UV-C, λ_{max} = 254 nm, manufactured by Philips, Holland). Minitab Software (Version 17) was employed to design the experiments and optimize the process using RSM.

Synthesis of Tin Dioxide Nanoparticles

First, 7.012 g of tin chloride pentahydrate has been dissolved in 100 mL of water. Next, it was placed inside the ultrasonic bath for 20 minutes and under 60 ˚C. Then, gradually ammonia solution was added drop by drop, until the pH would be regulated at 9.9. After 24 hours, the solution was passed from filter paper and the resultant sediments were washed out many times using water and ethanol. Finally, the intended sediments were dried up at 80 ˚C. Finally, it was calcinated at 400 ˚C.[25]

Aniline Polymerization in the Presence of Tin Dioxide Nanoparticles

Polymerization included the following stages:

1. Synthesis of aniline (0.1 M) solution in HCl through adding 0.46 mL of aniline to 50 mL of HCl and putting it on the agitator for 80 minutes.
2. Synthesis of APS solution (0.1M) through dissolving 1.14 g of APS in 50 mL of HCl and placing it on the agitator for 80 minutes.
3. Preparation of SnO_2 (0.1 M) solution through solving 0.75 g of the synthesized SnO_2 in 50 mL of HCl and placing it within an ultrasonic bath for a period of 90 minutes.

Then, the following stages for nanocomposite synthesis were performed:

50 mL of aniline was added wit 5 mL of SnO_2 solution was placed inside an ultrasonic bath for 90 minutes. Next, APS was slowly added to the solution. After 2 hours, green sediments were observed, the sediment was washed using HCl and put under room temperature in order to be dried up.[26]

Procedure of Cefixime Removal During the UV/PA-SnO_2/H_2O_2 Process

According to the experiment design, the experiments were carried out in the tubular reactor containing 4 L of antibiotic solution. After 15 min in darkness to reach the equilibrium, hydrogen peroxide in different contents was added to the solution, the UV-C lamp was then turned on. To create fluid flow through the reactor, a pump was used, and samples were taken at the specified times by the RSM. The effect of various parameters including reaction time, solution pH, antibiotic concentration, and hydrogen peroxide concentration on the removal efficiency was investigated.

By using a UV–Vis spectrophotometer (Shimadzu, UV mini-1240) the antibiotic concentration was measured at a wavelength of 286 nm, which is corresponded to the maximum absorbance. The amount of removal (R%) was calculated by using equation 1:

$$R(\%) = \frac{C_\circ - C_t}{C_\circ} \times 100 \quad (1)$$

Where C_0 and C_t are the initial and present concentrations

of the antibiotic in solution (mg/L), respectively.

According to Table 2, to optimize the process, the experimental design was implemented using the central composite design method ran in the Minitab software (Version 17). In the experimental design method, the experiments are designed in such a way that the factors are tested simultaneously for the achievement of the answer. The main design framework of the experiment is based on a series of standard schemes that consider the interaction between factors in order to affect each other. In this case, the final optimal point can be reached with a smaller number of experiments.[27]

Results and Discussion

SEM and TEM Images of Nanocomposite Surface

The SEM images of the nanocomposites have been shown in Figure 2. The porous structure of the crosslinked matrix was still present in the nanocomposites. Based on the images, the photocatalyst dispersion was homogeneous. The SEM images illustrated that the addition of SnO_2 nanoparticles to polyaniline synthesized under ultrasonic waves was encapsulated these particles inside the polymer coating. The chemical analysis by EDX coupled with ESEM was performed to confirm the dispersion of the photocatalyst in the sample. As can be seen from Figure 3, this analysis confirms the presence of carbon, oxygen, nitrogen and tin particles. The weight percentage of elements in the composition has been given in Table 3.

As can be seen from the TEM images in Figure 4, a polyaniline layer coated on SnO_2 particles was formed with a thickness in the range of 5 to 100 nm.

Table 2. Experimental Design Matrix for Experimental and Predicted Cefixime Removal

Coded Variables	Variable levels				
	-2	-1	0	+1	+2
Time (min) (X_1)	40	60	80	100	120
pH (X_2)	7	8	9	10	11
[H_2O_2] (mM) (X_3)	3.63	6.06	8.49	10.92	13.35
[Cefixime] (mg/L) (X_4)	10	20	30	40	50
Flow rate (L/min) (X_5)	0.67	0.82	0.97	1.12	1.27

Analysis of Mapping Images of the Nanocomposite

Figure 5 shows the elemental distribution maps with a resolution of 128×100. The two elements: C and N corresponding to the polymeric matrix are present in the complete image. On the other side, Sn is also homogeneously dispersed in the whole matrix indicating the presence of nanoparticles trapped in the polymer. The elemental distribution maps confirm the dispersion of the SnO_2 photocatalyst in the network of polyaniline. This suggests that the approach used for the synthesis of the nanocomposites promoted photocatalyst immobilization and homogeneous distribution.

Analysis of Fourier Transform-Infrared Spectrophotometer Taken From the PA/SnO_2 Nanocomposite

After washing and distillation, the FTIR spectrum of the nanocomposite was recorded through an ultrasonic approach. The FTIR spectrum of PA/SnO_2 nanocomposite has been shown in Figure 6. The tensile vibration of the aromatic C-H band was around 1117 cm^{-1} and the bending vibration of C-H bond was around 503 and 795 cm^{-1}. Furthermore, the tensile vibration of the C-N bond was evident in 1239 and 1296 cm^{-1} of benzene ring which is one of the distinctive features of pure Polyaniline. C-H

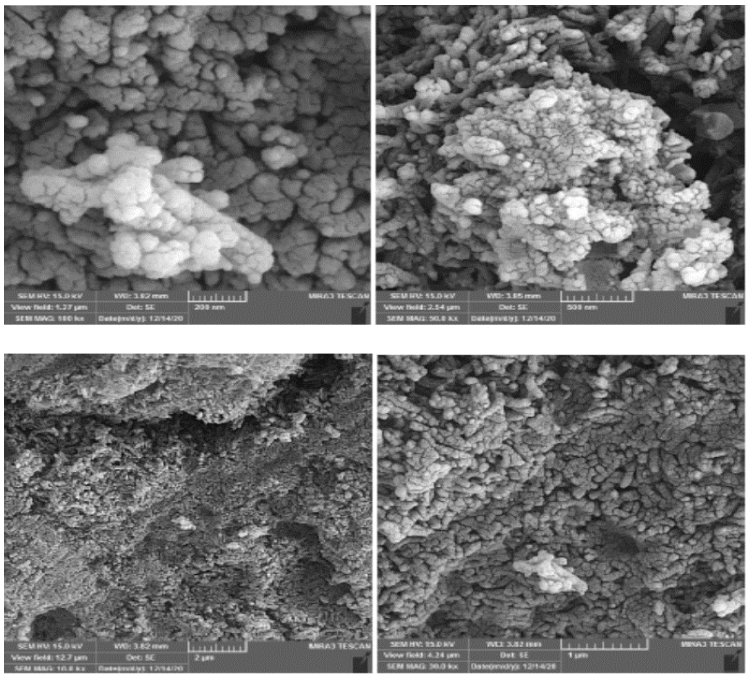

Figure 2. The SEM Images Taken From the Surface of the PA/SnO_2 Nanocomposite

modes are used as a method to identify the benzene ring in organic compounds. For example, C-H in ethylene with sp3 hybrid shows the absorption peak at 1117 cm^{-1} as well as the bending vibration of C-H in polyaniline. The low-intensity vibration around the 672 cm^{-1} region is related to the asymmetric state of Sn–O–Sn tin oxide. Absorption peaks at 791 cm^{-1} are a characteristic of the aromatic ring substitution from the para position, indicating the formation of a polymer. The absorption peak in 1464 and 1521 cm^{-1} corresponds to the C=C and C=N peaks of benzoid and quinoid rings, which indicate the oxidized state of polyaniline.[28] Therefore, the results illustrated that the two components of the nanocomposite are consistently present in the structure of the nanocomposite.

Table 3. The Weight Percentages (%wt) Obtained From the EDX Elemental Analysis of the PA/SnO_2 Nanocomposite

Elements	C	N	O	Sn
Weight percentage (%w)	49.76	33.71	15.33	1.20

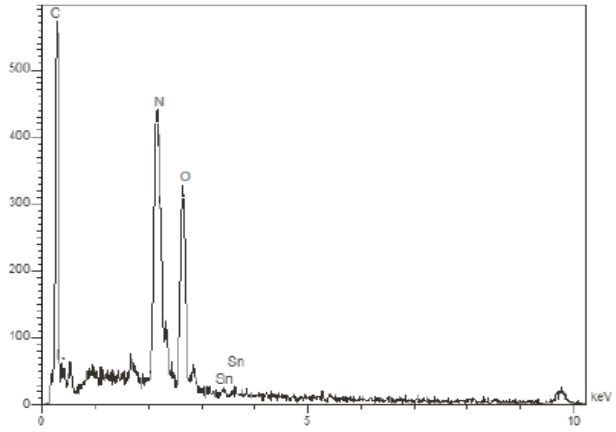

Figure 3. The EDX Image of the PA/SnO_2 Nanocomposite

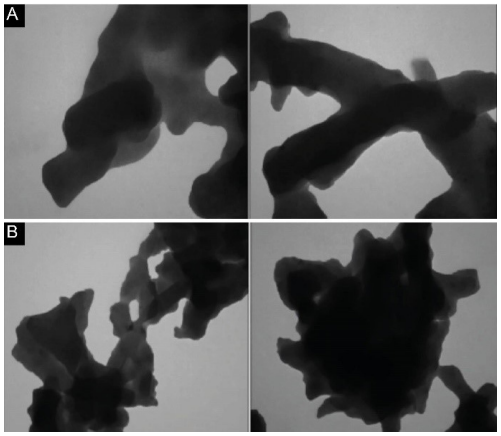

Figure 4. TEM Images of the PA/SnO_2 Nanocomposite: (A) 60 nm; (B) 150 nm

Evaluation of Thermal Gravimetric Analysis

Figure 7 shows the TGA curve of the PA and PA/SnO_2 nanocomposites. As shown in this Figure 7, the pure polyaniline TGA curve has a weight loss between 50 and 100 °C, which can be attributed to the removal of water or solvent. Weight loss from 250 to 610 °C can also be attributed to the degradation of the polymer structure and final decomposition has been accrued in 610 °C.[29] As can be seen, the PA/SnO_2 nanocomposite undergoes a slower decomposition, which includes 20% of mass reduction under 170 °C and 57% mass reduction under 650 °C. The data displays significant thermal stability of the PA/SnO_2 nanocomposite. A comparison between the TGA curve of the PA/SnO_2 nanocomposite with pure polyaniline and the destruction pattern of the nanocomposite suggests that the nanocomposite has higher thermal stability compared with pure polyaniline due to the presence of tin dioxide nanoparticles within its structure.

Optimization of the Process

According to Table 4, the optimization of the process was done by the Minitab software consisting of 32 experiments with one repetition. Giving the results of optimization data, Figure 8a was employed to observe the effect of each factor on the removal process. As can be seen, the higher slope of graph for each parameter determines a greater effect on the procedure; therefore, it can be said that all the mentioned parameters were effective in the process and played an essential role. Since a higher removal efficiency

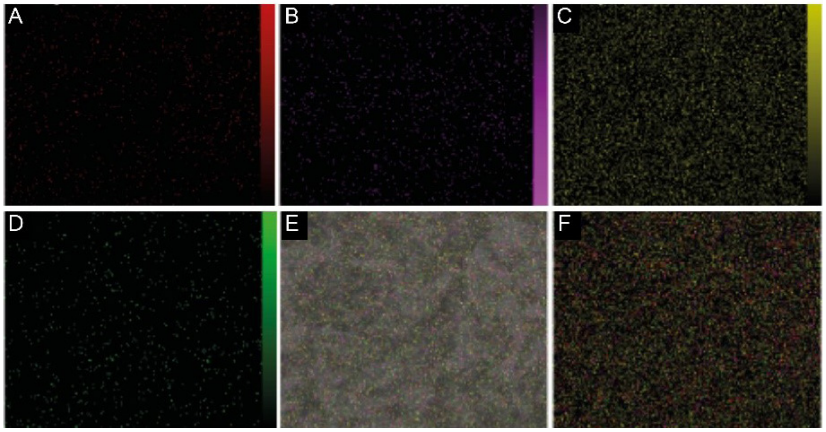

Figure 5. The Mapping Images Taken From the PA/SnO_2 Nanocomposite: (A) Oxygen, (B) Nitrogen, (C) Carbon, (D) Tin, (E & F) the Frequency Distribution of All Available Elements

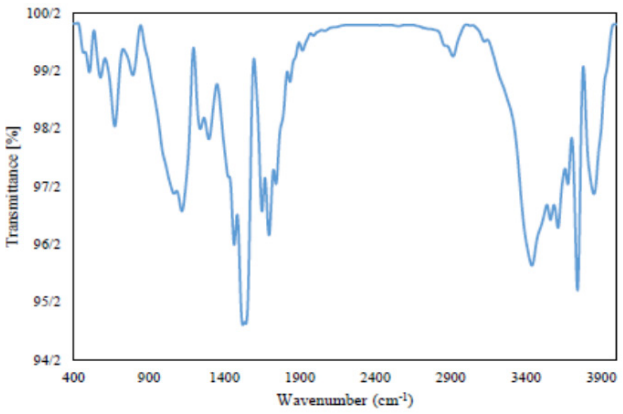

Figure 6. FT-IR Spectrum of the PA/SnO_2 Nanocomposite

was required, then any parameter displaying higher R% was more favorable. Hence, the pH of 8.69, time of 120 minutes, H_2O_2 concentration of 4.22 mM and flow rate of 1.25 L/min, in the antibiotic solution containing 22.92 mg/L of cefixime, were the optimal values.

As seen in the histogram diagram in Figure 8b, a Gaussian form exists, which indicates the normal population of data and the appropriate correctness of results. Likewise, in the normal probability plot, the dispersion of the points around the line is suitable, and means the normal validation. Besides, because two other charts does not follow any regular pattern, the data have high adequate accuracy.[27]

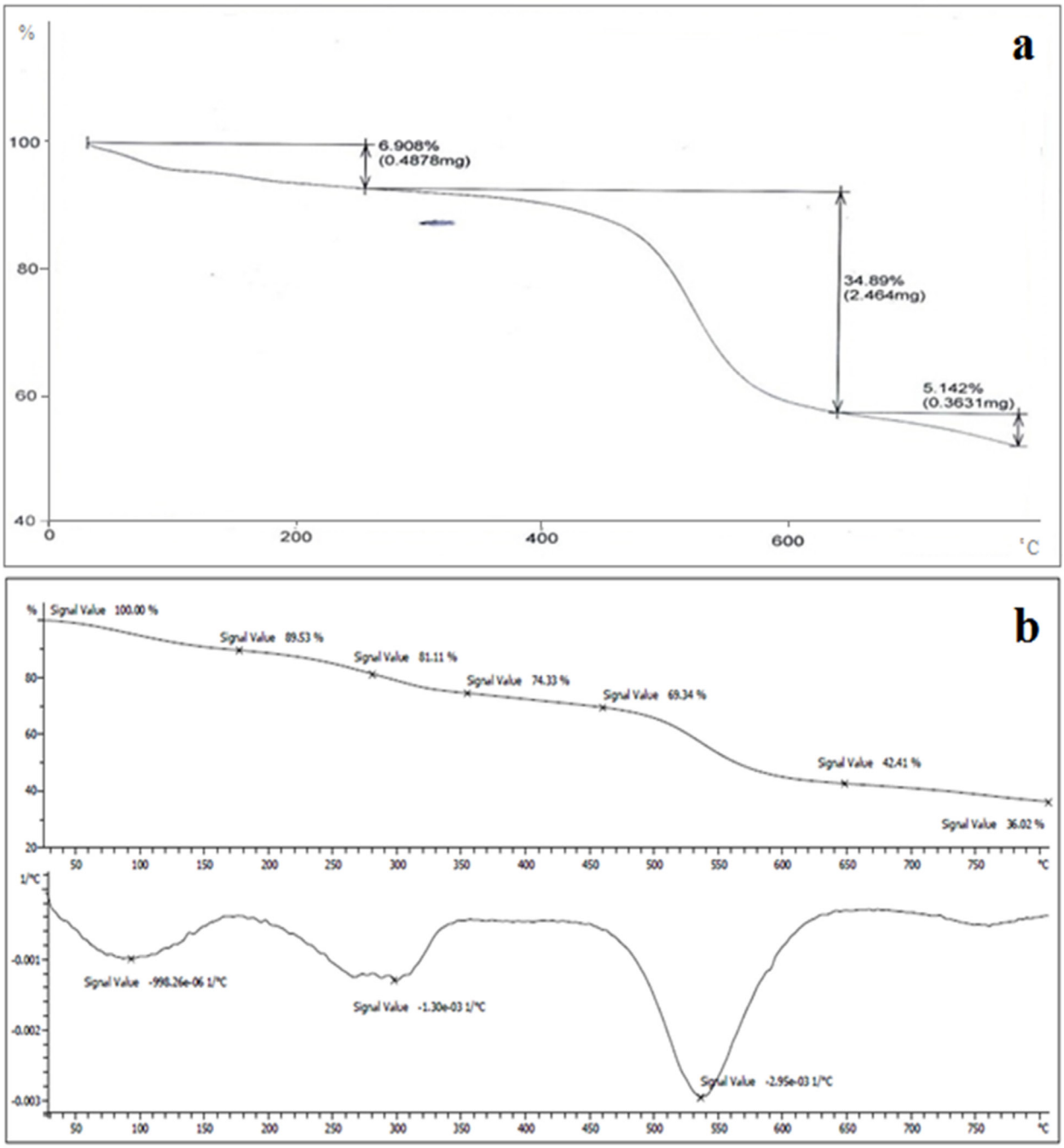

Figure 7. The TGA Curves of (a) PA and (b) PA/SnO_2 Nanocomposite

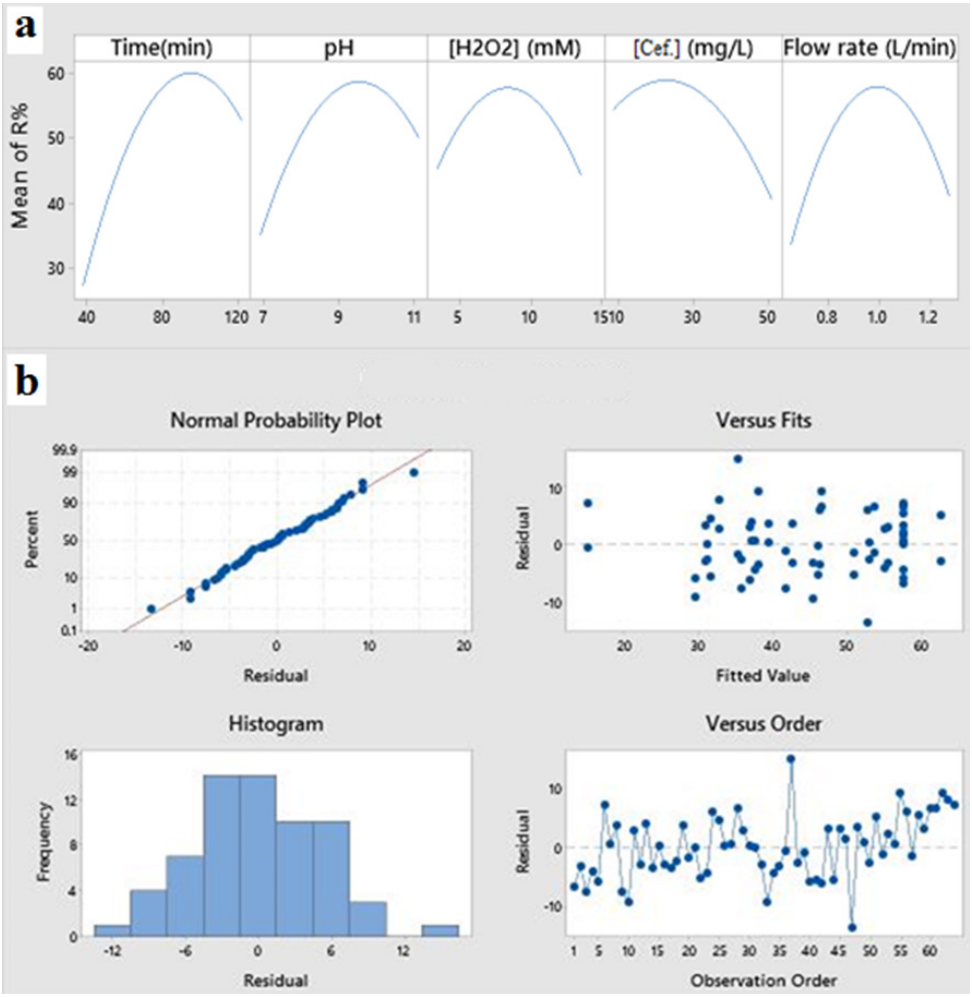

Figure 8. (a) The Efficiency Study of the Parameters in Antibiotic Removal Using the Photocatalytic Method (b) Residual Graphs to Data Accuracy Examination

Interactions Among the Factors Using Two and Three-Dimensional Diagrams

Based on the data and results from Table 4 related to optimization, the effect of each parameter on each other in removing cefixime contaminant is shown in the form of three-dimensional diagrams in Figure 9.

According to Figure 9a, the removal efficiency increases by increasing time. Also, in examining the effect of time and pH simultaneously, it is observed that, at low pH and high time, the highest removal efficiency can be achieved. The results showed that, with increasing process time, the number of hydroxyl radicals produced increases and thus the removal efficiency increases. As can be seen, with increasing pH from 7 to 10, the removal efficiency increases, but with increasing the pH too much, the removal efficiency decreases again. This phenomenon can be explained by the fact that, as the pH increases, the catalyst surface becomes negatively charged and the cefixime molecules are absorbed onto the catalyst surface through the acidic functional groups in their structure. This allows the molecules to participate in photocatalytic reactions and be decomposed. However, when the pH is raised beyond 10, the cefixime molecules are deprotonated and converted to anions, causing them to desorb from the negatively charged catalyst surface. As a result, the removal efficiency decreases

According to Figure 9b, it is observed that, with increasing the concentration of hydrogen peroxide, the removal efficiency increased, which can be expressed by the fact that, with increasing the concentration of hydrogen peroxide, the number of hydroxyl radicals increased, thereby enhancing the reaction between hydroxyl radicals and antibiotic molecules as well as improving the removal efficiency. However, with an increase of hydrogen peroxide from about 9 mm, due to the excessive increase of hydroxyl radicals and the possibility of their collision with each other, the active radicals are eliminated and the pollution removal efficiency declines.

As can be seen from Figure 9c, as the flow rate of the solution inside the reactor increased, the amount of photocatalytic degradation of the antibiotic increased, which can be explained by the fact that as the velocity of the fluid increased, the number of contaminant molecules colliding with the photocatalyst surface and the photocatalytic reactions of hydroxyl radicals with pollutant molecules increased at the catalyst surface. However, it appears that increasing the flow rate from approximately 1 L/min resulted in a decrease in contaminant removal efficiency. This may be due to the fact that an excessively high fluid flow rate in the reactor, beyond the optimal

Table 4. Value of variables in the optimization state of the experiments

Experiment number	Time (min)	pH	H_2O_2 concentration (mM)	Cefixime concentration (mg/L)	Flow rate (L/min)	R%
1	80	9	8.49	30	0.97	51.06
2	80	9	8.49	30	1.27	39.6
3	80	9	8.49	30	0.67	28.2
4	80	9	8.49	10	0.97	51
5	40	9	8.49	30	0.97	23.73
6	60	8	10.92	40	1.12	22.2
7	100	8	6.06	20	0.82	37.8
8	60	8	10.92	20	0.82	43.1
9	80	9	8.49	50	0.97	34.28
10	80	9	13.35	30	0.97	36.26
11	100	8	10.92	40	0.82	35.5
12	60	8	6.06	40	0.82	27.95
13	100	8	6.06	20	0.82	41.2
14	80	9	3.63	30	0.97	42.8
15	80	9	8.49	30	0.97	75.86
16	80	9	13.35	20	0.97	42.4
17	60	10	6.06	20	0.82	34.6
18	100	10	10.92	40	1.12	50.62
19	80	9	8.49	30	1.27	46.3
20	60	10	10.92	20	1.12	33.6
21	100	8	10.92	20	1.12	45.9
22	100	8	10.92	20	1.12	40.8
23	60	8	6.06	20	1.12	33.3
24	100	10	10.92	20	0.82	58.8
25	60	10	6.06	40	1.12	36.25
26	80	9	8.49	30	0.97	57.8
27	80	9	8.49	30	0.97	58.2
28	60	10	10.92	40	0.82	53.05
29	80	9	8.49	10	0.97	57.6
30	60	8	10.92	20	0.82	39.8
31	100	10	6.06	40	0.82	31.25
32	100	10	6.06	20	1.12	59.8
33	40	9	8.49	30	0.97	20.4
34	80	9	8.49	30	0.97	53.4
35	100	8	6.06	40	1.12	52.4
36	60	8	10.92	40	1.12	14.55
37	60	10	10.92	20	1.12	49.9
38	100	10	6.06	40	0.82	28.65
39	80	9	8.49	50	0.97	40.7
40	80	9	8.49	30	0.97	51.8
41	80	11	8.49	30	0.97	45.66
42	80	7	8.49	30	0.97	30.66
43	80	7	8.49	30	0.97	39.9
44	60	10	6.06	40	1.12	26.05
45	100	8	6.06	40	1.12	58.4
46	80	9	8.49	30	0.97	59
47	100	10	10.92	20	0.82	39.5
48	80	9	8.49	30	0.97	61
49	60	8	6.06	20	1.12	38.3
50	80	9	8.49	30	0.67	33
51	100	10	6.06	20	1.12	67.8
52	80	11	8.49	30	0.97	49.7
53	80	9	8.49	30	0.97	59.8
54	100	10	10.92	40	1.12	53.5
55	60	10	10.92	40	0.82	55.6
56	80	9	3.63	30	0.97	52.3
57	120	9	8.49	30	0.97	52.3
58	80	9	8.49	30	0.97	63
59	60	8	6.06	40	0.82	34
60	80	9	8.49	30	0.97	64
61	120	9	8.49	30	0.97	60.3
62	60	10	6.06	20	0.82	47.2
63	100	8	10.92	40	0.82	40.5
64	80	9	8.49	30	0.97	64.7

value, causes the antibiotic molecules to not have enough time to remain on the surface of the photocatalyst, thus preventing sufficient time for destructive reactions to occur.

In Figure 9d, it can be observed that the removal efficiency decreases at high initial antibiotic concentrations, while a low initial pollutant concentration with a longer process time can improve the removal efficiency. Given the fixed conditions of the other parameters, a certain amount of hydroxyl radicals significantly contribute to the removal process, thus reducing the initial contaminant concentration results in an increase in removal efficiency. In summary, it can be observed that a combination of a longer process time and lower initial pollutant concentration can result in an appropriate removal efficiency. Regarding Figures 9a-d, it can be observed that a combination of high H_2O_2 concentration, low antibiotic concentration, long reaction time, and high pH can enhance the removal efficiency due to their simultaneous effects.[30]

Prediction of the Optimal Conditions for Cefixime Removal

The Minitab software is capable of evaluating the results of optimization tests and identifying optimal values for each parameter to achieve the highest removal efficiency. That is, the program can predict the percentage of elimination that a given design will lead to. In fact, the purpose of experimental design, in any way, is to find the most optimal conditions with the least amount of time, cost and energy.

According to Figure 10, the program estimates that, if

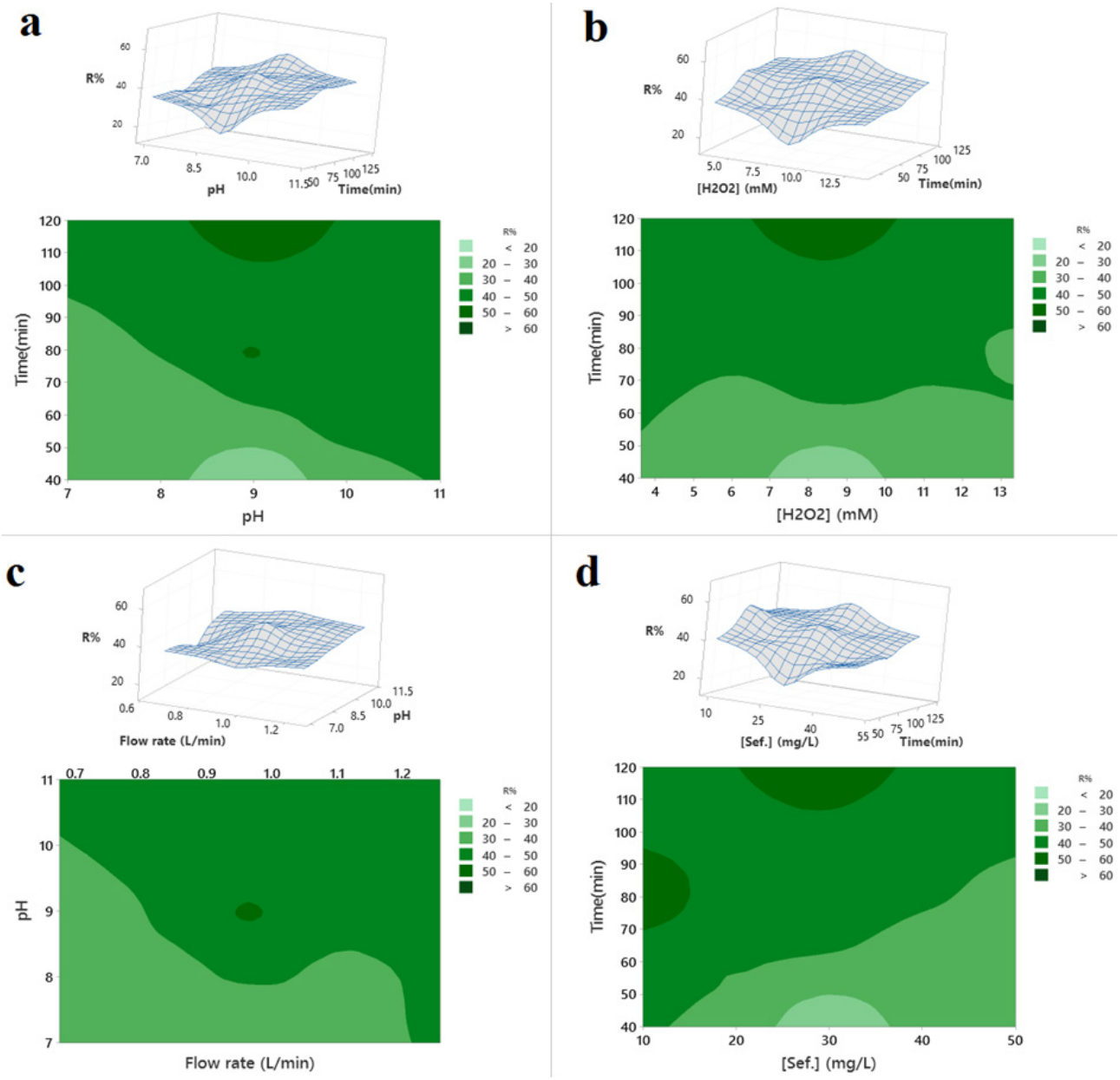

Figure 9. 2D and 3D Charts of the Effects of Various Factors on Cefixime Antibiotic Removal Using the Photocatalytic Method.

an experiment is performed with 95% confidence level in which the values of the parameters are: time of 120 minutes, pH of 8.69, hydrogen peroxide concentration of 4.22 mM, flow rate of 1.25 L/min and initial antibiotic concentration of 22.92 mg/L, then we will reach a removing efficiency of approximately 72%.

According to the similar works done in the photocatalytic degradation of cefixime antibiotic, the possible degradation mechanism has been reported in the Figure 11.[31]

Definition of Regression Equation

Based on the available optimization data, a regression equation can be used to predict the removal efficiency without conducting any experiments, thus providing a quick means to obtain the removal efficiency. The regression equation is as equation 2:

$$R\% = -439.5 - 0.151X_1 + 53.8\ X_2 + 8.69\ X_3 + 1.061\ X_4 + 373.1\ X_5 - 0.00998\ X_1\ X_1 - 3.421\ X_2\ X_2 - 0.498\ X_3\ X_3 - 0.02317\ X_4\ X_4 - 218.7\ X_5\ X_5 + 2.125\ X_1\ X_5 + 1.34\ X_2\ X_3 - 12.84\ X_3\ X_5$$

Where, X_1, X_2, X_3, X_4 and X_5 are time (min), pH, H_2O_2 concentration (mM) and antibiotic cefixime concentration (mg/L), respectively.

Figure 12 illustrates the graph of this equation, and validates the correctness and accuracy of the optimization experiments, where the axes x and y are predicted and experimental values, respectively. Thus, as shown in Figure 12, the distribution of experimental data around the predicted values is tight, indicating that the experiment process was conducted with minimal operator/device errors.

Figure 12 shows that the scatter of the experimental

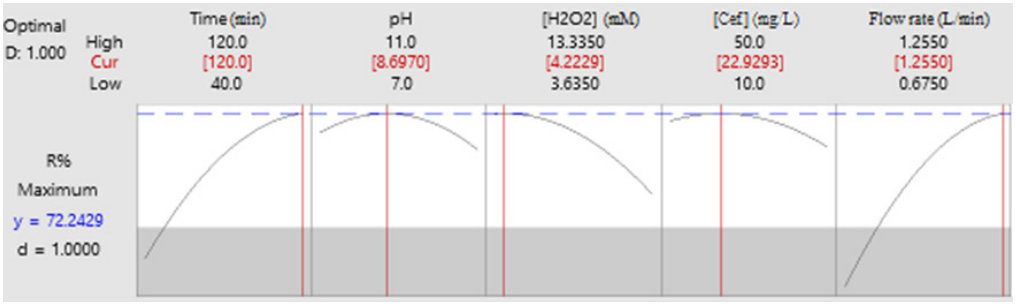

Figure 10. The Prediction Plots for Highest Cefixime Removal Using the Photocatalytic Approach

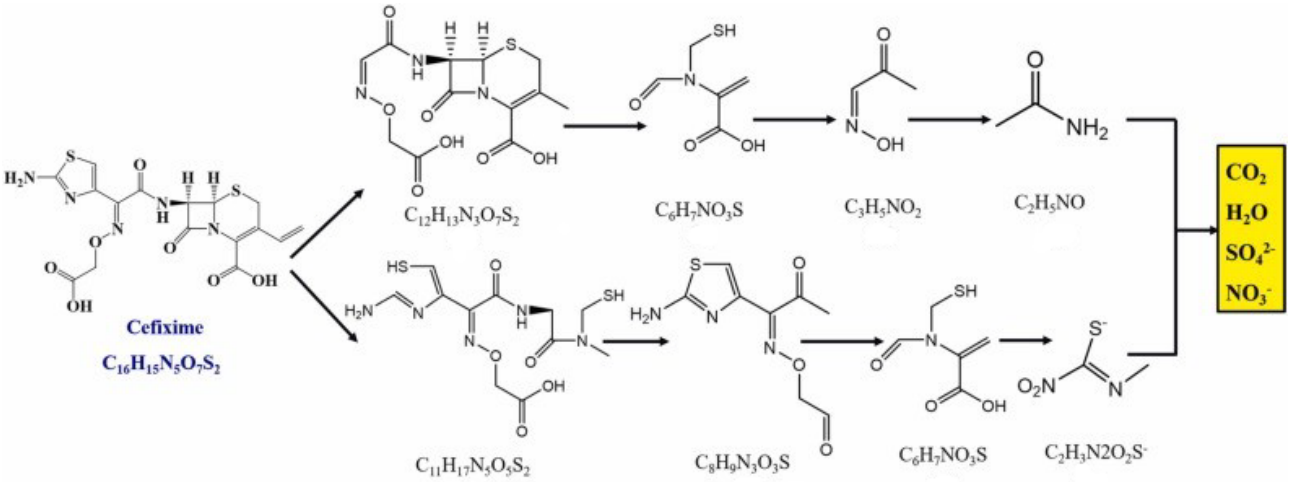

Figure 11. Possible Degradation Mechanism of the Process

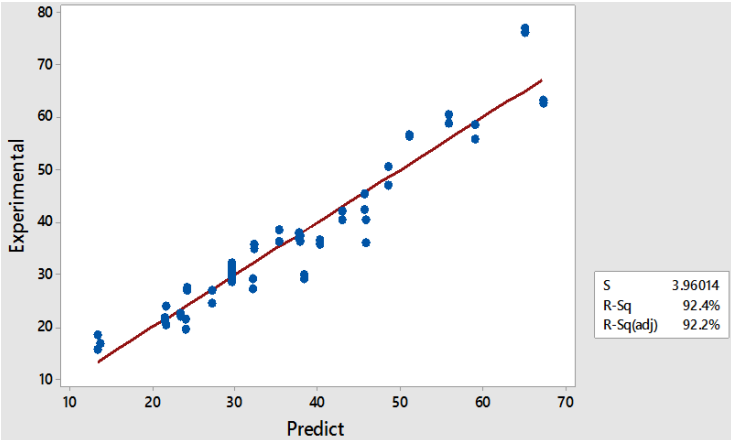

Figure 12. The Regression Plot for Cefixime Removal Using the Photocatalytic Procedure

results around the values predicted by the software are close to each other, indicating that the testing process was performed with minimal errors from the operator, device, and method. An ANOVA table was also presented to determine the reliability and validity of the experiments. According to Table 5, the data have acceptable validity.

Conclusion

In the present study, the PA/SnO_2 nanocomposite was prepared and used in the process of removing cefixime from contaminated water by a photocatalytic method. Using RSM for the optimization of the removal process, a practical removal efficiency of approximately 70% was achieved, demonstrating the acceptable proficiency of this method for the removal of cefixime antibiotic from wastewater. The amount of antibiotic contaminant removal is affected by pH, initial antibiotic concentration, process time, flow rate, and hydrogen peroxide concentration. The results of the optimization experiments showed that the pollutant degradation efficiency increased with increasing process time and pH. The optimal values were found to be a time of 120 minutes and a pH of 8.69. With increasing the amount of hydrogen peroxide and flow rate, the amount of removal increases and then decreases, Therefore, at the concentration of 4.22 mM, and the velocity of 1.25 L/min, the highest amount of removal of antibiotic cefixime was

Table 5. ANOVA Table Obtained From the Design Of The Experiments

Source	Adj SS	Adj MS	F Value	*P* Value
pH	1394	348.5	2.44	0.057
Time (min)	2847	711.7	6.02	0.000
[H_2O_2] (mM)	774.1	293.5	1.26	0.095
[Cef.] (mg/L)	735.3	290.7	1.19	0.101
Flow rate (L/min)	1349	337.3	2.35	0.065

achieved. Also, with increasing antibiotic concentration, the rate of antibiotic removal decreased. According to the prediction by the RSM using the Minitab software, a theoretical efficiency of 72% can be achieved via the optimal conditions.

Acknowledgments
This article was extracted from the MSc thesis of the first author approved by the Department of Chemistry, Islamic Azad University, Tabriz branch. The authors would like to thank the Research Council for their generous support of this research.

Authors' Contribution
Conceptualization: Kambiz Seyyedi.
Data curation: Kambiz Seyyedi.
Formal analysis: Kambiz Seyyedi.
Funding acquisition: Kambiz Seyyedi.
Investigation: Parishan Salih Mohammed.
Methodology: Kambiz Seyyedi.
Project administration: Kambiz Seyyedi.
Resources: Parishan Salih Mohammed.
Software: Parishan Salih Mohammed.
Supervision: Kambiz Seyyedi.
Validation: Kambiz Seyyedi.
Visualization: Parishan Salih Mohammed.
Writing–original draft: Parishan Salih Mohammed.
Writing–review & editing: Kambiz Seyyedi.

Competing Interests
The authors declared no conflict of interest.

Ethical Approval
There were no ethical considerations to be considered in this research.

Funding
This study was partially supported by Tabriz Branch of Islamic Azad University.

References
1. de Carvalho Costa LR, de Moraes Ribeiro L, Hidalgo GE, Féris LA. Determination of optimal operating parameters for tetracycline removal by adsorption from synthetic and real aqueous solutions. J Environ Sci Health A Tox Hazard Subst Environ Eng. 2020;55(14):1615-23. doi: 10.1080/10934529.2020.1829887.
2. Bayan EM, Pustovaya LE, Volkova MG. Recent advances in TiO_2-based materials for photocatalytic degradation of antibiotics in aqueous systems. Environ Technol Innov. 2021;24:101822. doi: 10.1016/j.eti.2021.101822.
3. Russell JN, Yost CK. Alternative, environmentally conscious approaches for removing antibiotics from wastewater treatment systems. Chemosphere. 2021;263:128177. doi: 10.1016/j.chemosphere.2020.128177.
4. Çelekli A, Al-Nuaimi AI, Bozkurt H. Adsorption kinetic and isotherms of Reactive Red 120 on *Moringa oleifera* seed as an eco-friendly process. J Mol Struct. 2019;1195:168-78. doi: 10.1016/j.molstruc.2019.05.106.
5. Elami D, Seyyedi K. Removing of carmoisine dye pollutant from contaminated waters by photocatalytic method using a thin film fixed bed reactor. J Environ Sci Health A Tox Hazard Subst Environ Eng. 2020;55(2):193-208. doi: 10.1080/10934529.2019.1673089.
6. Tuerk J, Sayder B, Boergers A, Vitz H, Kiffmeyer TK, Kabasci S. Efficiency, costs and benefits of AOPs for removal of pharmaceuticals from the water cycle. Water Sci Technol. 2010;61(4):985-93. doi: 10.2166/wst.2010.004.
7. Wei Z, Liu J, Shangguan W. A review on photocatalysis in antibiotic wastewater: Pollutant degradation and hydrogen production. Chinese J Catal. 2020; 41:1440-1450. doi: 10.1016/S1872-2067(19)63448-0.
8. Akbari MZ, Xu Y, Lu Z, Peng L. Review of antibiotics treatment by advance oxidation processes. Environm Adv. 2021;5:100111. doi: 10.1016/j.envadv.2021.100111.
9. Chakraborty S, Roy M, Saha R. Cost-effective synthesis method of facile environment friendly SnO_2 nanoparticle for efficient photocatalytic degradation of water contaminating compound. Water Sci Technol. 2020;81(3):508-17. doi: 10.2166/wst.2020.130.
10. Bagheri F, Chaibakhsh N. Efficient visible-light photocatalytic ozonation for dye degradation using Fe2O3/MoS2 nanocomposite. Sep Sci Technol. 2021;56(17):3022-32. doi: 10.1080/01496395.2020.1861018.
11. Roguai S, Djelloul A. Elaboration, characterization and applications of SnO_2, 2 %Gd-SnO_2 and 2 %Gd-9 %F-SnO_2 thin films for the photocatalytic degradation of MB by USP method. Inorg Chem Commun. 2022;138:109308. doi: 10.1016/j.inoche.2022.109308.
12. Alagarasi A, Rajalakshmi PU, Shanthi K, Selvam P. Solar-light driven photocatalytic activity of mesoporous nanocrystalline TiO_2, SnO_2, and TiO_2-SnO_2 composites. Mater Today Sustain. 2019;5:100016. doi: 10.1016/j.mtsust.2019.100016.
13. Tammina SK, Mandal BK, Kadiyala NK. Photocatalytic degradation of methylene blue dye by nonconventional synthesized SnO_2 nanoparticles. Environ Nanotechnol Monit Manag. 2018;10:339-50. doi: 10.1016/j.enmm.2018.07.006.
14. Costa LN, Nobre FX, Lobo AO, Elias de Matos JM. Photodegradation of ciprofloxacin using Z-scheme TiO_2/SnO_2 nanostructures as photocatalyst. Environ Nanotechnol Monit Manag. 2021;16:100466. doi: 10.1016/j.enmm.2021.100466.
15. Asgari E, Esrafili A, Jonidi Jafari A, Rezaei Kalantary R, Farzadkia M. Synthesis of TiO_2/polyaniline photocatalytic nanocomposite and its effects on degradation of metronidazole in aqueous solutions under UV and visible light radiation. Desalin Water Treat. 2019;161:228-42. doi: 10.5004/dwt.2019.24291.
16. Faraji M, Najafi Moghadam P, Hasanzadeh R. Fabrication of binder-free polyaniline grafted multiwalled carbon nanotube/TiO_2 nanotubes/Ti as a novel energy storage electrode for supercapacitor applications. Chem Eng J. 2016;304:841-51. doi: 10.1016/j.cej.2016.07.034.
17. Li J, Peng T, Zhang Y, Zhou C, Zhu A. Polyaniline modified SnO_2 nanoparticles for efficient photocatalytic reduction of aqueous Cr(VI) under visible light. Sep Purif Technol. 2018;201:120-9. doi: 10.1016/j.seppur.2018.03.010.
18. Sayed MA, Ahmed MA, El-Shahat MF, El-Sewify IM. Mesoporous polyaniline/SnO_2 nanospheres for enhanced photocatalytic degradation of bio-staining fluorescent dye from an aqueous environment. Inorg Chem Commun. 2022; 139:109326. doi:10.1016/j.inoche.2022.109326.
19. Sandhya J, Kalaiselvam S. UV responsive quercetin derived and functionalized CuO/ZnO nanocomposite in ameliorating photocatalytic degradation of rhodamine B dye and enhanced biocidal activity against selected pathogenic strains. J Environ Sci Health A Tox Hazard Subst Environ Eng. 2021;56(8):835-

48. doi: 10.1080/10934529.2021.1930770.
20. Arora R. Nanocomposite polyaniline for environmental and energy applications. Mater Today Proc. 2021;44:633-6. doi: 10.1016/j.matpr.2020.10.603.
21. Zia J, Riaz U. Photocatalytic degradation of water pollutants using conducting polymer-based nanohybrids: a review on recent trends and future prospects. J Mol Liq. 2021;340:117162. doi: 10.1016/j.molliq.2021.117162.
22. Karpuraranjith M, Thambidurai S. Design and synthesis of graphene-SnO_2 particles architecture with polyaniline and their better photodegradation performance. Synth Met. 2017;229:100-11. doi: 10.1016/j.synthmet.2017.02.017.
23. Swati, Saini M, Anupama, Shukla R. Investigation of structural, thermal, and electrical properties of magnesium substituted cobalt ferrite reinforced polyaniline nanocomposites. Ceram Int. 2021;47(23):33835-42. doi: 10.1016/j.ceramint.2021.08.295.
24. National Center for Biotechnology Information. PubChem Compound Summary for CID 5362065, Cefixime. 2022. Available from: https://pubchem.ncbi.nlm.nih.gov/compound/Cefixime.
25. Majumdar S, Devi PS. Synthesis of SnO_2 nanoparticles using ultrasonication. AIP Conf Proc. 2010;1276(1):1-7. doi: 10.1063/1.3504298.
26. Silva ALC, Ugucioni JC, Correa S, Ardisson JD, Macedo WAA, Silva JP, et al. Synthesis and characterization of nanocomposites consisting of polyaniline, chitosan and tin dioxide. Mater Chem Phys. 2018;216:402-12. doi: 10.1016/j.matchemphys.2018.06.025.
27. Afshar Moghaddam M, Seyyedi K. Optimization of the Sunset Yellow dye removal by electrocoagulation using a response surface method. Water Sci Technol. 2022;85(1):206-19. doi: 10.2166/wst.2021.500.
28. Senthilkumar S, Rajendran A. Synthesis, characterization and electrical properties of nano metal and metal-oxide doped with conducting polymer composites by in-situ chemical polymerization. MOJ Polym Sci. 2017;1(6):192-5. doi: 10.15406/mojps.2017.01.00031.
29. Mostafaei A, Zolriasatein A. Synthesis and characterization of conducting polyaniline nanocomposites containing ZnO nanorods. Prog Nat Sci. 2012;22(4):273-80. doi: 10.1016/j.pnsc.2012.07.002.
30. Zhang Y, Zhao YG, Maqbool F, Hu Y. Removal of antibiotics pollutants in wastewater by UV-based advanced oxidation processes: influence of water matrix components, processes optimization and application: a review. J Water Process Eng. 2022;45:102496. doi: 10.1016/j.jwpe.2021.102496 .
31. Zhao Y, Ji C, Wang Y, Liang X, Fan J. Green and efficient degradation of cefixime by 3D flower-like BiOBr: performance and degradation pathway. Colloids Surf A Physicochem Eng Asp. 2022;635:128024. doi: 10.1016/j.colsurfa.2021.128024.